



Contents lists available at ScienceDirect

International Journal of Infectious Diseases

journal homepage: [www.elsevier.com/locate/ijid](http://www.elsevier.com/locate/ijid)



## Spatial–temporal patterns of dengue in areas at risk of dengue hemorrhagic fever in Kaohsiung, Taiwan, 2002

Tzai-Hung Wen<sup>a,b</sup>, Neal H. Lin<sup>b</sup>, Day-Yu Chao<sup>b,c</sup>, Kao-Pin Hwang<sup>d,e</sup>, Chih-Chun Kan<sup>f</sup>, Katherine Chun-Min Lin<sup>g</sup>, Joseph Tsung-Shu Wu<sup>b</sup>, Scott Yan-Jang Huang<sup>g</sup>, I-Chun Fan<sup>h</sup>, Chwan-Chuen King<sup>b,\*</sup>

<sup>a</sup> Department of Geography, College of Science, National Taiwan University, Taipei, Taiwan

<sup>b</sup> Graduate Institute of Epidemiology, College of Public Health, National Taiwan University, Taipei, Taiwan

<sup>c</sup> Graduate Institute of Veterinary Public Health, National Chung Hsing University, Taichung, Taiwan

<sup>d</sup> Division of Pediatric Infectious Disease, Department of Pediatrics, Kaohsiung Medical University, Kaohsiung, Taiwan

<sup>e</sup> Department of Pediatrics, Chang Gung Memorial Hospital, Kaohsiung, Taiwan

<sup>f</sup> Graduate Institute of Life Sciences, National Defense Medical Center, Taipei, Taiwan

<sup>g</sup> Department of Public Health, College of Public Health, National Taiwan University, Taipei, Taiwan

<sup>h</sup> Center for Geographic Information Science, Academia Sinica, Taipei, Taiwan

### ARTICLE INFO

#### Article history:

Received 28 August 2008

Received in revised form 20 April 2009

Accepted 2 June 2009

**Corresponding Editor:** William Cameron, Ottawa, Canada.

#### Keywords:

Dengue

Space–time clustering

Viral hemorrhagic fever

Spatial epidemiology

Geographic information systems

Vector-borne infectious disease

### SUMMARY

**Objective:** This study aimed to examine whether spatial–temporal patterns of dengue can be used to identify areas at risk of dengue hemorrhagic fever (DHF).

**Methods:** Three indices – probability of case-occurrence, mean duration per wave, and transmission intensity – were used to differentiate eight local spatial–temporal patterns of dengue during the 2002 epidemic in Kaohsiung, Taiwan. DHF densities (DHF cases/km<sup>2</sup> per 100 dengue cases) in each spatial–temporal typed area were compared.

**Results:** Areas with three high indices correlated with the highest DHF density: (1) high transmission intensity only; (2) long duration of wave only, and (3) high transmission intensity plus long duration of wave. However, cumulative incidences of dengue cases were not correlated with DHF densities.

**Conclusion:** Three spatial–temporal indices of dengue could provide useful information to identify areas at high risk of DHF.

© 2009 International Society for Infectious Diseases. Published by Elsevier Ltd. All rights reserved.

## 1. Introduction

Disease mapping can be used to pinpoint the areas where outbreaks originate and effectively target high-risk areas for early prevention and control.<sup>1,2</sup> Geographical information systems (GIS) and statistical analysis of spatial characteristics of a disease have made it possible to detect the clustering of cases and link the clustering dynamics with geographical locations that carry certain risk factors favorable for the sources of infection (e.g., mosquito breeding sites) and for the spread of infection (e.g., vector exposure).<sup>3–5</sup> Recent studies have mapped risk areas over different defined time periods to describe the temporal dynamics of epidemics.<sup>6–10</sup> However, few studies have integrated spatial and temporal factors to compare the spread of the milder form of

dengue (dengue fever (DF)) and the more severe form (dengue hemorrhagic fever (DHF)) and to differentiate the risk patterns of an epidemic involving total dengue cases versus DHF cases.

The clinical manifestations of dengue include DF, DHF, and the most severe and potentially fatal dengue shock syndrome (DSS). It has been shown that more DHF cases emerge from a dengue/DHF epidemic in endemic and hyper-endemic areas, which often correlates to more fatalities, especially if patients obtain medical care too late or the cases are managed inappropriately.<sup>11</sup> However, because not all epidemics of dengue involve DHF,<sup>12</sup> it would help save lives if we knew the epidemiological conditions associated with the emergence of severe epidemics involving more DHF cases and the overall risk patterns of total dengue cases.

Dengue virus, a flavivirus with four antigenically distinct serotypes, is transmitted mainly by *Aedes aegypti* and *Aedes albopictus* in Taiwan. GIS-based studies have mapped spatial clustering patterns of dengue cases and have analyzed the association between these patterns and relevant entomological

\* Corresponding author. Tel.: +886 2 3322 8034; fax: +886 2 2351 1955.  
E-mail address: [chwanchuen@gmail.com](mailto:chwanchuen@gmail.com) (C.-C. King).

factors<sup>2,6,8</sup> and environmental conditions,<sup>13</sup> and have identified the spatial–temporal diffusion patterns of dengue and vector distributions.<sup>6–8,14</sup> Although these studies have helped us understand the mechanism of dengue epidemics, none, to the best of our knowledge, have analyzed the different spatial–temporal conditions related to the emergence of DHF cases in a severe epidemic of dengue/DHF.

Most epidemics of dengue in Taiwan have started with imported cases.<sup>15</sup> The 2001–2003 epidemic of dengue/DHF in Kaohsiung, Taiwan, was the largest and the most severe epidemic in that two-city area in 60 years.<sup>16</sup> This DHF-laden epidemic has made it possible to investigate the temporal and spatial emergence of severe DHF cases within an epidemic. Instead of relying on annual incidence to simply describe the epidemic, we used a spatial risk model integrating various temporally defined epidemiological characteristics of that outbreak to identify the temporal risk factors that might be related to potential severity of dengue epidemics involving more DHF cases.

## 2. Materials and methods

### 2.1. Study areas and study populations

From May of 2001 to March of 2003, Kaohsiung City and a satellite city, Fengshan City, suffered the largest epidemic of dengue in Taiwan since 1943.<sup>16</sup> In order to compare the annual cumulative incidence of dengue with the other three temporal risk indicators, we analyzed the major epidemic period during the 2002 calendar year (January 1 to December 31 of 2002) with a total of 4790 confirmed dengue cases (98.3% of the 2001–2003 epidemic) (Figure 1). All the dengue cases were laboratory confirmed by molecular identification,<sup>17</sup> serological diagnosis,<sup>18</sup> or virus isolation.<sup>19</sup> Using criteria set by the World Health Organization (WHO), there were 4504 DF cases and 286 DHF cases from April to December 2002 (Figure 1). In this study, we aggregated the 4321 confirmed dengue cases with complete and accurate addresses (90.2% of total cases) to the basic administration unit 'Li' in Taiwan, then mapped by using ArcGIS 9.1 (ESRI, Inc., Redlands, CA, USA), and further analyzed risk patterns of the dengue epidemic in the 2002 epidemic period.

### 2.2. Spatial and temporal units used to characterize the studied dengue cases

This study used 'Li', the smallest local governing unit in Taiwan, as the mapping unit to spatially characterize variations in case-

distribution and a '7-day week' as the temporal unit, which is the aggregated unit used by Taiwan's Centers for Disease Control (Taiwan CDC) in their routine surveillance reporting systems. Most urban areas of Li covered 0.26–0.58 square kilometers, and had 2100–5300 people and 850–1600 households.<sup>20</sup> In total, we aggregated the Li-specific 4321 dengue cases and mapped them into the total 423 Li units in 52 weeks of the 2002 year. Taiwan CDC provided all the confirmed DF and DHF cases in each Li without personal identifiers.

### 2.3. The three temporally defined indices as epidemiological measures

This study used temporally defined epidemiological characteristics, which we recently developed into population-oriented risk indices,<sup>21</sup> to measure both the magnitude and severity of a dengue epidemic. These three temporal indices were: (1) probability of occurrence ( $\alpha$ ), which we defined as the probability that the total number of weeks with one or more dengue cases occurred during the entire epidemic period (total 52 weeks in 2002); (2) duration of epidemic ( $\beta$ ), which we defined as the mean number of weeks per epidemic wave when cases successively occur, which means a time of disease occurrence marked before and after by no reported dengue cases; and (3) intensity of transmission ( $\gamma$ ), which we defined as the mean incidence of cumulative dengue cases occurring in consecutive weeks per epidemic wave that had persisted for more than two weeks. The total number of epidemic waves during the entire epidemic period was calculated as the sum of waves when dengue cases occurred continuously over weeks. Microsoft Excel was used to calculate the values of all the three temporal indices from the case data. Based on the above calculation of temporally defined indices for each Li unit, we transformed the annual cumulative dengue cases into the three temporal indices (occurrence, duration, and intensity) for each Li and generated the Li-specific choropleth maps with these various temporal index values to be compared with that of cumulative incidence, which is the annual incidence rate during the total 52 weeks of 2002.

### 2.4. Classification of the five population risk levels based on integrating spatial autocorrelation of each of the three temporal risk indices

Spatial autocorrelation refers to the degree of the association between the spatial location of a testing variable and its neighbors.<sup>29</sup> There are spatial autocorrelations while the values of the variable are interrelated spatially, which also means there

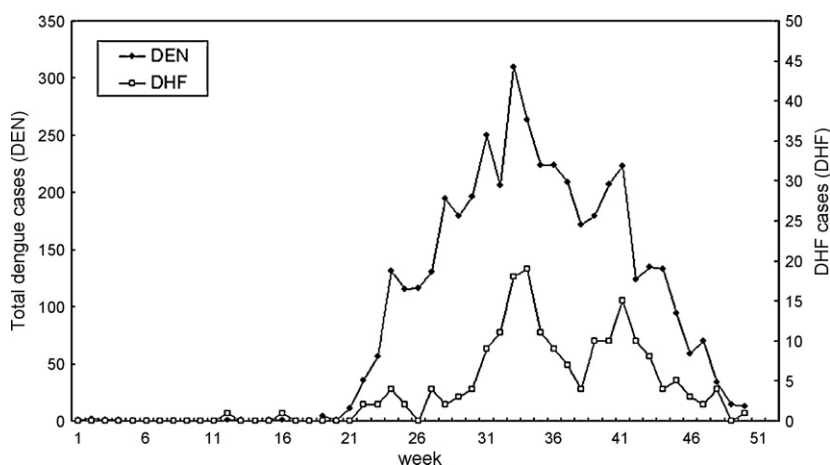


**Figure 1.** The epidemic curve of weekly total confirmed dengue and dengue hemorrhagic fever (DHF) cases for Kaohsiung and Fengshan cities (i.e., the two-city area), 2002. This area covered 85.1% of total dengue cases in Taiwan (4790/5630) from January to December, 2002.

are spatial patterns to those correlations.<sup>23</sup> Details are described in Appendix A. In this study, we determined the spatial autocorrelations of the three temporal indices and used the local indicator of spatial autocorrelation (LISA) as a spatial risk index to identify significant spatial patterns, including clustering and outliers.<sup>23</sup> The definition of a LISA index is:

$$I(i) = \frac{(X_i - \bar{X})}{\delta} \times \sum_{j=1}^n W_{ij} \times \frac{(X_j - \bar{X})}{\delta} \quad (1)$$

where  $I(i)$  = the LISA index for region  $i$ , and  $W_{ij}$  = the proximity of region  $i$  to region  $j$ , where a value of 1 means the region  $i$  is next to the region  $j$ .  $X_i$  is the value of a temporal index for region  $i$ ,  $X_j$  is the value of a temporal index for region  $j$ ,  $\bar{X}$  is the mean of the tested temporal index for the whole tested regions,  $\delta$  is the standard deviation of the tested temporal index  $X$ , and  $n$  is the total number of regions (in Li units) to be evaluated. The term  $(X_i - \bar{X}) \times (X_j - \bar{X})$  describes the degree of similarity in a testing temporal index within a specific area and its neighbors. Thus, each of the three temporal indices for the 2002 dengue epidemic in the two-city area was evaluated.

The null hypothesis for LISA was that a temporal index distributed spatially without a defined pattern. Therefore, we employed a Monte Carlo significance test, which calculates the likelihood a cluster would emerge by chance within a given population, to evaluate the statistical significance of its spatial pattern. The LISA value of each tested temporal index (incidence,  $\alpha$ ,  $\beta$ , and  $\gamma$ ) was considered statistically significantly high with a 95% confidence interval. Using LISA index values and one index at a time, we classified risk areas into the five epidemiologically distinct and statistically significant risk levels, from the highest to the lowest.

**Level 5 (extreme risk):** If both a target area and its neighboring areas had higher values for one of the temporal indices tested, the target area was considered to have a statistically significant 'positive LISA index value' and was regarded to be at 'extreme risk' (Figure 2a).

**Level 4 (high risk):** When a target area had a lower value of a tested temporal index than those of its neighboring areas, the target area was considered to have a statistically significant 'negative LISA index value' and was viewed to be at 'high risk' (Figure 2b).

**Level 3 (moderate risk):** If a target area had a higher value of a tested temporal index than those of its neighboring areas, the target area was considered to have a statistically significant 'negative LISA index' but was judged to be at 'moderate risk', because it would pose some risk to its neighbors (Figure 2c).

**Table 1**  
Classification of all eight possible risk types defined by the three temporal indices

Risk type	Three epidemiologically defined temporal indices		
	Occurrence index, $\alpha^a$	Duration index, $\beta^a$	Intensity index, $\gamma^a$
Hi-ODI	High <sup>b</sup>	High <sup>b</sup>	High <sup>b</sup>
Hi-OD	High <sup>b</sup>	High <sup>b</sup>	–
Hi-O	High <sup>b</sup>	–	–
Hi-DI	–	High <sup>b</sup>	High <sup>b</sup>
Hi-I	–	–	High <sup>b</sup>
Hi-OI	High <sup>b</sup>	–	High <sup>b</sup>
Hi-D	–	High <sup>b</sup>	–
Hi- $\phi$	–	–	–

<sup>a</sup> Three temporal indices are occurrence probability, epidemic duration and intensive transmission.

<sup>b</sup> 'High' means the value of that indicated temporal index is statistically significant high ( $p < 0.05$ ).

**Level 2 (mild risk):** If a target area and its neighbors had sporadic cases without significant spatial patterns, meaning the tested temporal index of the target area was neither particularly higher or lower than its neighboring areas, the LISA index of the tested temporal index in this target area was not statistically significant and that area was considered to be at 'mild risk' (Figure 2d).

**Level 1 (low risk):** If both the target area and its neighbors had low temporal index values, the target area had the lowest risk cluster of the tested temporal index and was considered to be at 'low risk' (Figure 2e).

2.5. Spatial risk types based on combinations of the three temporal indices

To determine the risk profile of an area, the LISA maps for each of the three temporal indices were overlaid on each other, and each Li unit was classified as having one of eight possible risk types as defined by the values of the three temporal indices: (1) Hi-ODI: statistically significantly high for all three indices, occurrence (O), duration (D), and intensity (I); (2) Hi-OD: significantly high for occurrence and duration; (3) Hi-DI: significantly high for duration and intensity; (4) Hi-OI: significantly high for occurrence and intensity; (5) Hi-O: significantly high only for occurrence; (6) Hi-D: only duration high; (7) Hi-I: significantly high only for intensity; and (8) Hi- $\phi$ : no high values for all three temporal indices ( $\alpha$ ,  $\beta$ ,  $\gamma$ ) reaching statistical significance (Table 1). For example, the risk type for one area would be classified as 'Hi-ODI' if its values of all  $\alpha$ ,  $\beta$ , and  $\gamma$  indices were statistically significantly high.

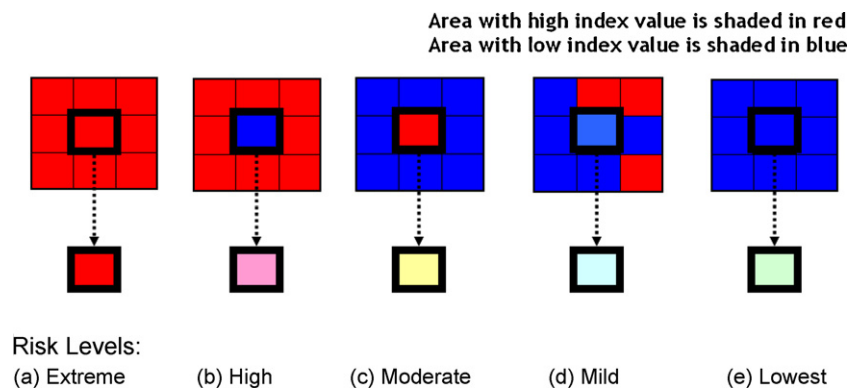


**Figure 2.** Definition of five spatial risk levels. Areas with high values of the tested index are shown as red, and areas with low index values are shaded in blue. Five spatial risk levels include: (a) extremely high, (b) high, (c) moderate, (d) mild, and (e) low. Among these spatial risk distributions, (a) is the spatial clusters of high value of the tested temporal index, (b) and (c) are the spatial outliers, (d) is the spatial random distribution of the tested temporal index, and (e) is spatial clusters with low values of the tested temporal index.

## 2.6. Overall analyses of risk patterns using integrated spatial and temporal data

We analyzed all Li-specific spatial and temporal risk indicators for the 2002 dengue/DHF epidemic in Kaohsiung as measured by: (1) weekly occurring probability over one year ( $\alpha$ ), (2) mean duration per epidemic wave ( $\beta$ ), and (3) transmission intensity ( $\gamma$ ) per epidemic wave. All three epidemiologically related temporal indices ( $\alpha$ ,  $\beta$ ,  $\gamma$ ) and cumulative incidence were mapped independently for each Li-area, and the risk patterns were compared. We then examined the association between the risk patterns of dengue cases and the severe epidemic involving DHF cases in 2002.

## 2.7. The two indices to evaluate the magnitude vs. severity of a dengue epidemic

To investigate the conditions for each of the above risk types involving total dengue cases versus the emergence of DHF, we used two evaluation indices representing magnitude and severity of an epidemic: (1) cumulative incidence of dengue cases (DEN/POP) and (2) the total dengue normalized DHF density (abbreviation: DHF density). DEN/POP is as the annual cumulative incidence rate of all confirmed dengue cases in the year of 2002 in Kaohsiung. This index denotes the magnitude of an epidemic. DHF density is the number of DHF cases per square kilometer area to the total confirmed dengue cases, and denotes the severity of an epidemic.

## 3. Results

### 3.1. Spatial–temporal patterns of the 2002 dengue cases in Kaohsiung using the three temporal indices versus incidence rate

#### 3.1.1. Mapping occurrence, duration, and intensity

We used the three temporal indices ( $\alpha$ ,  $\beta$ , and  $\gamma$ ) as well as incidence rate to retrospectively map the spatial patterns of dengue cases and to identify possible risk areas visually for the 2002 dengue epidemic (seen in Figure 3, in terms of occurrence (Figure 3.2), duration (Figure 3.3), and intensity (Figure 3.4)). The two areas with the highest cumulative incidence indicated by the darkest area (Figure 3.1) were (1) a location between the boundaries of Kaohsiung and Fengshan cities (also known as two-city areas) and (2) a location within the central part of Fengshan City. These two areas showed different temporal patterns by visual examination. In addition to these two areas, we also found another area within Kaohsiung's Sanmin District with longer duration (Figure 3.3c) and the area located in Zuoyin District (Figure 3.4c) in Kaohsiung with higher transmission intensity. However, the cumulative incidences in these two districts were all low (2.76/10 000 and 5.12/10 000, respectively), indicating that these three indices (Figure 3.2–3.4) did not correlate very well with the cumulative incidence (Figure 3.1).

#### 3.1.2. Size of risk areas of the three temporal indices versus annual incidence identified by spatially significant patterns

We identified statistically significant spatial patterns by using cumulative incidence and the three temporal indices plus LISA statistics to characterize spatial risk during this epidemic. The areas colored red in Figure 4 were the statistically significant clusters of extreme risk (e.g., the highest risk levels). Figure 4(A) shows two significant clusters of high incidence – (a) and (b): (a) areas covered 9.83 km<sup>2</sup> for 21 Li units and had 1302 dengue cases with an incidence rate of 21.1/1000 and (b) areas covered 1.05 km<sup>2</sup> for 9 Li units and had 256 dengue cases with an incidence rate of 18.3/1000. In these two clusters, each temporal index covered different sizes and numbers of Li units. Occurrence probability ( $\alpha$ )

involved 14.35 km<sup>2</sup> for 57 Li units in cluster (a) vs. 4.25 km<sup>2</sup> for 23 Li units in cluster (b) (Figure 4(B)). The mean duration per wave ( $\beta$ ) contained 8.74 km<sup>2</sup> of 28 Li units for (a) vs. 0.47 km<sup>2</sup> of 4 Li units for (b) (Figure 4(C)). Intensity ( $\gamma$ ) covered 4.24 km<sup>2</sup> for 17 Li units in (a) vs. 0.26 km<sup>2</sup> for 3 Li units in (b) (Figure 4(D)). Comparing the areas for the three temporal indices versus incidence rates, both (a) and (b) had similar high cumulative incidence (21.1/1000 vs. 18.3/1000), but they had very different temporal risk patterns shown by these three temporal indices. Although cluster (b) had 9 Li units with high incidence rates of dengue, this cluster illustrated only 4 Li units with longer durations ( $\beta$ ), 3 Li units with high intensities ( $\gamma$ ), and 23 Li units with high occurrence ( $\alpha$ ) (Table 2 and Figure 4).

### 3.2. Risk types of dengue using the combined three temporal indices

The LISA maps of the three temporal indices for each Li were overlaid on top of each other. Combining the statistically significant high values ( $p < 0.05$ ) of the three indices ( $\alpha$ ,  $\beta$ ,  $\gamma$ ) allowed us to classify all the studied Li units into eight risk types (Table 1, Figure 5). We investigated the spatial risks for all these risk types. In the Hi-ODI areas, 13 of 52 weeks (25.5% (= 0.255)), ( $\alpha$ ), had confirmed cases of dengue. Additionally, the mean duration ( $\beta$ ) was longer than one month ( $4.6 \pm 3.32$  weeks per epidemic wave), and the mean intensity ( $\gamma$ ) was  $3.2 \pm 2$  dengue cases per 10 000 people per wave (Table 3).

Other risk types had lower values for the three temporal indices than those in Hi-ODI. In the risk types with two indices being significantly higher, the values of occurrence and mean duration in Hi-OD were 0.24 and 2.91, and the mean values of duration and intensity in Hi-DI were 2.08 and 2.19. In the risk types with one index being significantly higher, the value of occurrence in Hi-O was 0.18, of mean duration in Hi-D was 2.13, and of intensity in Hi-I was 3.07, showing that each index value alone can still be very high, particularly the duration and intensity indices (Table 3). In the case of least risk (e.g., Hi- $\phi$ ), in which no statistically significant spatial–temporal relationship was identified, the values of the three temporal indices were lowest with 0.064 for occurrence, 1.13 for mean duration, and 0.58/10 000 for intensity. Interestingly, no area in this epidemic was of the high-occurrence, high-intensity, but low-duration risk type (Hi-OI).

### 3.3. Evaluation of the magnitude versus severity of the 2002 dengue/DHF epidemic in Kaohsiung

To investigate the relationship between population density and the spatial–temporal characteristics among all risk types (Table 1) and to better portray the severity of this epidemic in the two-city areas of Kaohsiung, we employed two evaluation indices, (1) DEN/POP and (2) DHF density, to uncover the trends in the dengue epidemics. With regard to DEN/POP, areas with the Hi-ODI risk type showed the greatest cumulative incidence (12.73) (Table 4).

However, with regards to DHF density (indicating the severity of dengue/DHF epidemic involving more DHF cases), areas of the Hi-I and Hi-D types with denser populations ( $> 23 000$  persons/km<sup>2</sup>), had higher values of DHF density at 7.62% and 6.04% (Table 4), respectively. DHF cases in these densely populated areas were associated more with either longer duration ( $\beta = 2.134 \pm 0.79$  weeks/wave) or higher intensity ( $\gamma = 3.074 \pm 2.17$  cases/10 000 population-at-risk/wave). These results suggested that duration per wave was an important factor for the severity of the epidemic. On the other hand, the highest DHF density (8.86%) was in areas of the Hi-DI risk type (Table 4), where population density was fewer than 2700 people/km<sup>2</sup>, and both higher transmission intensity ( $\gamma = 2.19$  cases/10 000 population-at-risk/wave) and longer duration ( $\beta = 2.08$  weeks/wave) (Table 3) presented with severe epidemic of dengue involving more DHF cases.

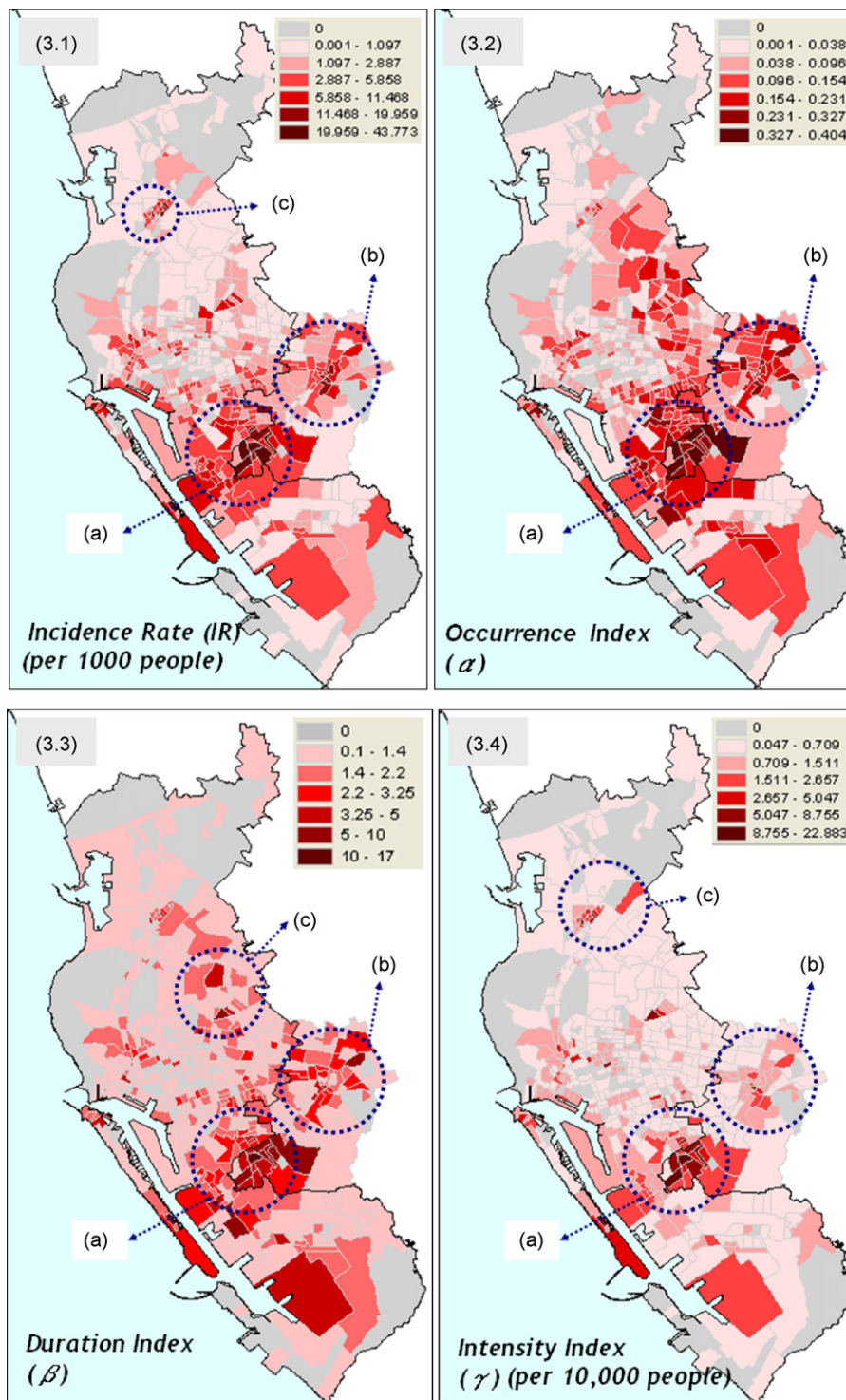


**Figure 3.** Mapping the values of incidence and the other three temporal indices (occurrence probability, epidemic duration, and intensive transmission) with observed clusters. The darker areas reflect a higher value of that indicated index. The locations of dengue clusters are shown as circled areas.

**4. Discussion**

This study used limited data sources, our three newly developed temporal indices (occurrence, duration, and intensity), and straightforward statistical methods in integrating and analyzing spatial-temporal epidemiological characteristics of different risk types, to identify potentially neglected areas of dengue virus transmission and to assess the overall magnitude versus potential severity of a dengue epidemic involving emer-

gence of more DHF cases. Public health officials at both local and national health agencies can easily apply the methods we developed from this study to focus more on risk areas that have longer duration per wave and higher transmission intensity.

Using the spatial patterns from the three temporal indices, more effective control strategies can be devised in those risk areas with various public health implications. For example, in the Hi-OD risk type (green color in Figure 5), control strategies may have minimized the transmission intensity in areas that had longer

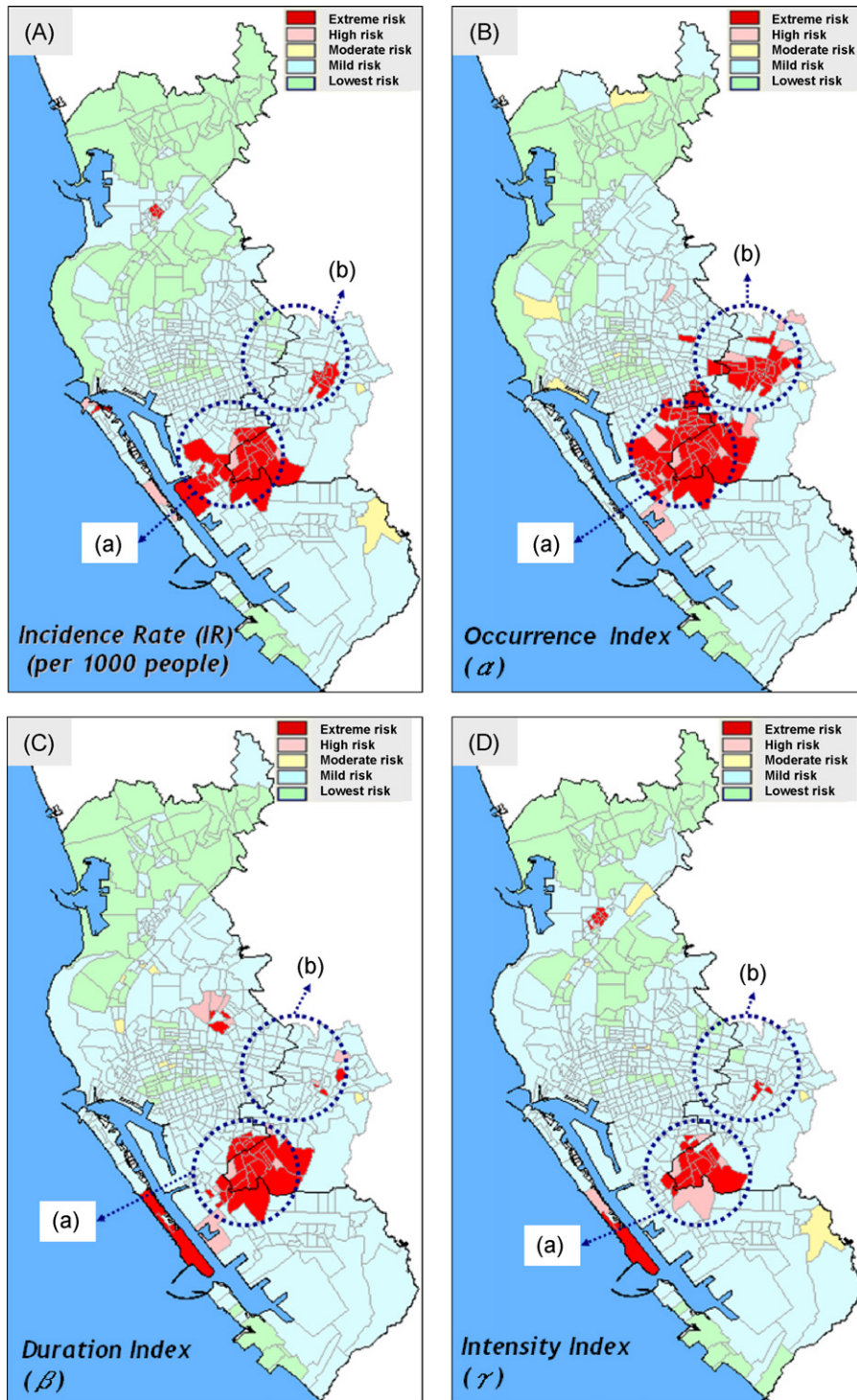


**Figure 4.** Dengue significant risk maps of incidence and the other three temporal indices to show spatial clusters and outliers. The local indicator of spatial autocorrelation (LISA) was adopted as the spatial risk index to identify both significant spatial clusters and outliers of the tested temporal indices. The Monte Carlo significance test was used to evaluate the statistical significance of spatial clusters and outliers with  $p < 0.05$ .

epidemic waves with more occurrences of the dengue cases. Meanwhile, Hi-D areas (purple color in Figure 5), where mosquito breeding sites may have been overlooked, may not have been identified as risk areas based on cumulative incidence alone. As a result, the continuous presence of mosquitoes could explain the extended duration in these areas. Conversely, in Hi-I areas, there was high intensity but low occurrence and low duration of the dengue cases, suggesting that control strategies had effectively broken the transmission and prevented further spread of dengue

virus. Hi-ODI areas were often surrounded by Hi-OD and Hi-O areas, which appeared mostly in the middle and late stages of the overall epidemic curve (Figure 6(a)). These clearly defined spatially differential patterns suggested that the epidemic might have initiated from those Hi-ODI centering areas where high intensity was important, then to the surrounding outer areas with Hi-OD, followed by the furthest outer areas with Hi-O. In addition, the failure to control outbreaks in Hi-ODI areas made it possible for dengue to gradually spread to other Hi-O areas (Figure 6(a)) and

**Table 2**

Comparisons of the two statistically significant clustering areas<sup>a</sup> – area (a) and area (b) located on the boundaries of Kaohsiung and Fengshan cities and the central part of the city of Fengshan, respectively using the three temporal indices

Area	Cumulative incidence			Occurrence ( $\alpha$ )			Duration ( $\beta$ )			Intensity ( $\gamma$ )		
	No. Li	Area (km <sup>2</sup> )	Index value	No. Li	Area (km <sup>2</sup> )	Index value	No. Li	Area (km <sup>2</sup> )	Index value	No. Li	Area (km <sup>2</sup> )	Index value
(a)	29	9.83	10.1–22.5	57	14.35	0.1–0.4	28	8.74	1.8–16.8	17	4.24	0.8–22.9
(b)	9	1.05	8.5–19.1	23	4.25	0.1–0.3	4	0.47	0.7–1.5	3	0.26	0.2–1.2

<sup>a</sup> Significant clusters means the spatial areas with extreme risk, indicating that both a target area and its neighboring areas had higher values for one of the temporal indices tested (areas colored red in Figure 4).

Hi-I areas (Figure 6(b)). Temporally, an ODI-to-OD-to-O pattern of transmission (Figure 6(a)) was found at the middle and later stages of the overall epidemic curve. This pattern was identified after evaluating Hi-ODI, Hi-OD and Hi-O risk types. In addition, we were able to visualize the emergence of Hi-D and Hi-I areas that were at a higher risk in having more DHF cases (Table 4). These areas were located further away from the epidemic foci, which were characterized by the Hi-ODI-to-OD-to-O risk types, and they also occurred later in the epidemic wave (Figure 6(b)). This pattern suggested that dengue infection had already spread beyond the foci, either by mosquito or by people who had mild or no clinical symptoms.

Traditional use of incidence data cannot distinguish the spatial differences in risk areas from those of their neighboring areas, which is crucial to the effective control of vector-borne infectious diseases. For example, ‘moderate risk’ was identified if a target area had a statistically significant higher value of a temporal index than

that of its neighboring areas (Figure 2(c)). In this study, several areas were spatially identified as ‘moderate risk’ (yellow areas in Figure 4(C) and 4(D)), but their target areas had higher  $\beta$  or  $\gamma$  values for the two temporal indices (i.e., duration and intensity) than the surrounding areas (target vs. surroundings:  $\beta = 1.5\sim 3.1$  vs.  $0.03\sim 0.6$  weeks/wave,  $\gamma = 1.04\sim 2.01$  vs.  $0.01\sim 0.57$  dengue cases/10 000 population-at-risk/wave), suggesting that these moderate risk areas were in fact potential future sources of transmission for subsequent epidemic waves. On the other hand, values of temporal index integrated with spatial epidemiology can provide more important information on time and place than incidence data alone for earlier prevention. For example, if the neighboring areas had a higher temporal index value than the target area of interest, it indicates that imminent outbreak in this area would happen if adequate prevention measures were not taken.

Local public health authorities can use the method developed from this study by integrating these three temporal indices with the levels of spatial risk to monitor dengue cases in a wider regional range, and to evaluate and improve their control measures in a more targeted way. We retrospectively constructed the risk map (Figure 5) marked with eight risk types (Table 3) and found that several risk areas may be overlooked due to low cumulative incidence (Figure 4). Using the cumulative incidence as the only measure of monitoring, several areas with significantly high risks (Hi-DI and Hi-D) were not identified. Transmission through patients with mild disease can perpetuate subsequent waves of the epidemic that was very likely due to low awareness because of low incidence. In addition, the dengue virus moved quickly from high-risk areas to surrounding neighborhoods, accelerated the epidemic to peak during the 2002 summer vacation time. In fact, the risk patterns for this dengue epidemic showed that the number of dengue cases and higher DHF densities in risk types Hi-D and Hi-I (Table 4) were located away from the epidemic foci (Figure 5), and peaked after the summer (Figure 6(b)), suggesting that infected persons in the epidemic foci spread the virus beyond the mosquito’s normal or usual flying range<sup>16</sup>. A transmission pattern such as this with long distances could be related to population movement<sup>7</sup>. Past dengue epidemics in Taiwan usually peaked in

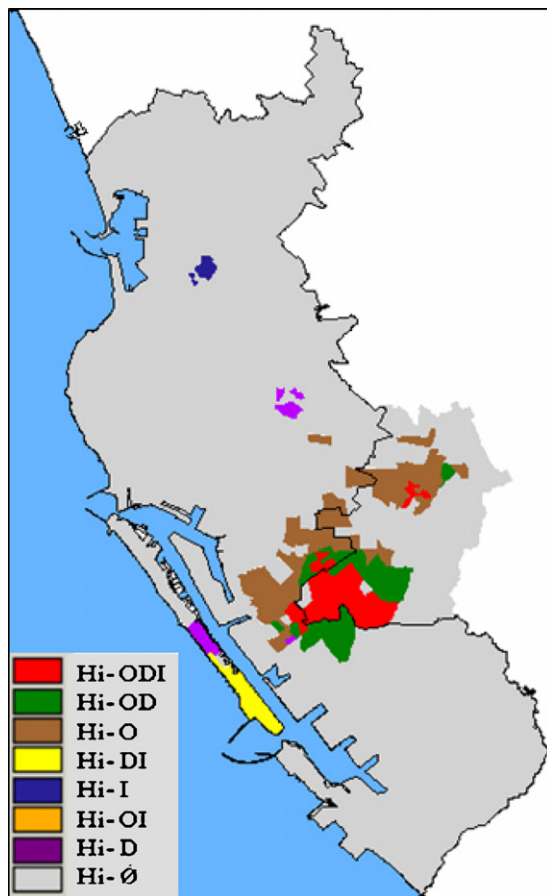


**Figure 5.** Mapping the eight different temporal-spatial risk types for the 2002 dengue epidemic in the two cities of the Kaohsiung area. Eight risk types were defined from all the possible combinations of high or low values of the three temporal indices (occurrence probability, epidemic duration, and intensive transmission).

**Table 3**

The mean  $\pm$  standard deviation values of the each of the three temporal indices for the eight possible risk types

Risk types	Mean $\pm$ standard deviation of the three temporal indices		
	Occurrence index ( $\alpha$ )	Duration index ( $\beta$ )	Intensity index ( $\gamma$ )
Hi-ODI	0.255 $\pm$ 0.08 <sup>a</sup>	4.608 $\pm$ 3.32 <sup>a</sup>	3.179 $\pm$ 2.01 <sup>a</sup>
Hi-OD	0.241 $\pm$ 0.08 <sup>a</sup>	2.919 $\pm$ 1.56 <sup>a</sup>	2.047 $\pm$ 2.47
Hi-O	0.183 $\pm$ 0.06 <sup>a</sup>	1.943 $\pm$ 0.73	1.173 $\pm$ 1.21
Hi-DI	0.106 $\pm$ 0.06	2.085 $\pm$ 0.83 <sup>a</sup>	2.191 $\pm$ 1.28 <sup>a</sup>
Hi-I	0.110 $\pm$ 0.05	1.925 $\pm$ 0.91	3.074 $\pm$ 2.17 <sup>a</sup>
Hi-OI	–	–	–
Hi-D	0.100 $\pm$ 0.04	2.134 $\pm$ 0.79 <sup>a</sup>	1.270 $\pm$ 1.44
Hi- $\phi$	0.064 $\pm$ 0.06	1.133 $\pm$ 0.83	0.585 $\pm$ 0.79

<sup>a</sup> The value is statistically significantly high ( $p < 0.05$ ).

**Table 4**  
Geographical characteristics, population density and evaluation of dengue risk for the eight risk types by the two indices (DEN/POP and DHF density)

Risk types	Regional characteristics				No of dengue cases			Evaluation indices	
	Number of Li <sup>a</sup>	Area (km <sup>2</sup> ) <sup>b</sup>	Population <sup>b</sup>	Population density (person/km <sup>2</sup> ) <sup>b</sup>	DEN <sup>c</sup>	DF <sup>c</sup>	DHF <sup>c</sup>	DEN/POP <sup>d</sup>	DHF density
Hi-ODI	20	4.503	82 765	18 380	1054	1011	43	12.73	0.91
Hi-OD	11	4.649	47 594	10 237	332	320	12	6.98	0.78
Hi-O	49	9.447	164 219	17 383	720	690	30	4.38	0.44
Hi-DI	2	1.556	4250	2731	29	25	4	6.82	8.86
Hi-I	10	0.419	11 301	26 971	94	91	3	8.31	7.62
Hi-OI	–	–	–	–	–	–	–	–	–
Hi-D	5	1.057	25 054	23 703	47	44	3	1.87	6.04
Hi-φ	445	172.924	1 481 952	8570	2045	1955	90	1.38	0.03
Total	542	194.56	1 817 135	9340	4321	4136	185	–	–

<sup>a</sup> Li is the basic administration unit in Taiwan for planning, implementation and election.

<sup>b</sup> The data of area and population were from the *General report the 2000 census of population and housing Taiwan-Fukien area, Republic of China* of the Directorate General of Budget, Accounting and Statistics (DGBAS).

<sup>c</sup> DEN: total number of confirmed dengue cases (dengue fever (DF) + dengue hemorrhagic fever (DHF)); POP: number of population.

<sup>d</sup> Two evaluation indices are DEN/POP and DHF density. DEN/POP is the Li-based annual incidence of all confirmed dengue cases per 1000 population-at-risk; DHF density is the Li-based number of DHF cases per square kilometer among total dengue cases as a measure of severity of the epidemic.

November after the rainy season (May to October). In this epidemic, however, humans infected before the summer of 2002 facilitated the spread of the virus from Hi-ODI and Hi-OD areas to other areas (Figure 6) as the extrinsic incubation period of mosquitoes was shorter during the warmer months of summer vacation period<sup>25</sup>.

The unique findings of this study show that epidemiological measures can be used to identify high risk areas more effectively,

which assists in optimizing resources and minimizing DHF cases worldwide. In the 2002 Kaohsiung epidemic, several neighborhoods with the Hi-DI, Hi-I and Hi-D risk types had the highest DHF density (Table 4), but were probably overlooked by public health officials because their incidence rates were low. Notably, in areas with these three risk types, dengue cases, particularly DHF cases, emerged in later waves after the peak and even at the tail end of the epidemic curve (Figure 6(b), Table 4). The late emergence of DHF

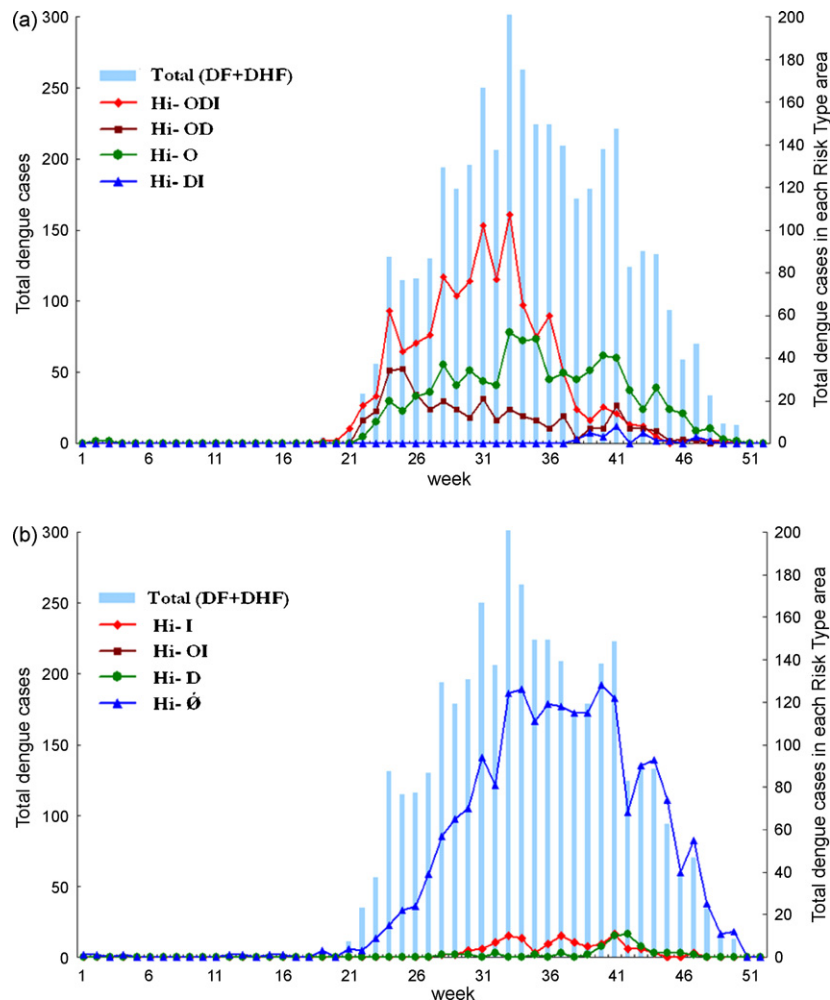


**Figure 6.** Epidemic curves of weekly total confirmed dengue cases in areas with each of the eight different risk types.

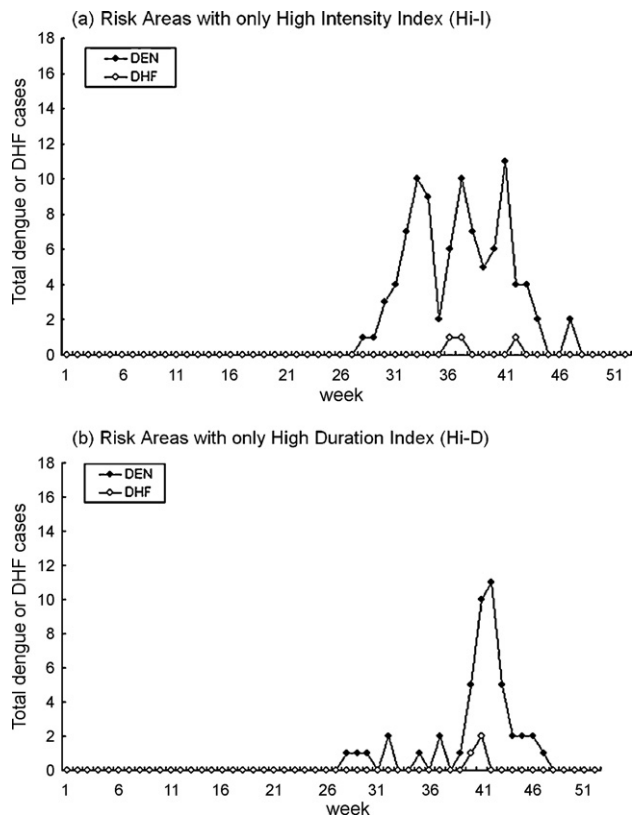


**Figure 7.** Epidemic curves of weekly total confirmed dengue (solid circles) versus DHF cases (empty circles) in areas with only high duration index (Hi-D) and only high intensity index (Hi-I).

cases after wide spreading, particularly in low incidence areas, may make it more difficult to implement control efforts in these areas. However, the longer duration in Hi-DI and Hi-D would probably create a potential to cause more phenotypic variations of quaspecies of dengue viruses (data not shown), similar to our observation in a previous epidemic,<sup>26</sup> which might have led to more DHF cases, even though the total number of dengue cases at the end of the outbreak period declined (Figure 7). Therefore, shortening the duration in the initial stages of an epidemic would reduce the risk of more DHF cases emerging in later stages. Although we observed that the longer duration and/or higher transmission intensity were associated with the emergence of more DHF cases from this study, the causal inference that these two conditions might lead to further DHF cases needs future prospective studies to prove.

The importance of duration index can be further demonstrated in those dengue endemic or hyper-endemic countries,<sup>2,7,8,10,11</sup> where persistent transmission of dengue virus at the population level to the end of the epidemic season could continue to transmit the virus during winter months through patients with milder symptoms. Most of these patients may not be identified because the epidemic is assumed to be over or nearly over, but they may significantly contribute to an epidemic in the next season, including more DHF cases in many parts of the world.<sup>27</sup> Another factor that can prolong or reignite an epidemic is that *Aedes albopictus* mosquitoes can remain active in winter and continue to infect humans beyond a dengue season.<sup>28</sup> The number of fatal DHF cases has grown in recent years in Southeast Asia, where control efforts seem to be failing. The increasing dengue severity between years is often overlooked, but the risk mapping methods described in this study could be used to proactively reduce and prevent these severe cases.

In conclusion, this study provides public health authorities with a more sophisticated tool to differentiate risk patterns of a dengue epidemic using three additional temporal indices rather than relying on annual cumulative incidence alone, so that high-risk areas can be comprehensively identified early in the epidemic based on their integrated spatial-temporal profiles. The method also directs broader perspectives on the temporal risks within the epidemic curves and emphasizes surveillance efforts at the tail end of an epidemic period. We believe this spatial-temporal model could be generalized to other infectious diseases such as epidemics of West Nile encephalitis in North America, Ebola hemorrhagic fever in Africa, and highly pathogenic avian influenza virus (HPAI) H5N1 that now threatens the world.<sup>29</sup>

### Conflict of interest

No conflict of interest to declare.

### Acknowledgements

We sincerely thank the staff of Kaohsiung City, the Kaohsiung County health bureaus and the Centers for Disease Control in Taiwan (Taiwan CDC) for their efforts in surveillance and vector control during the hard times of the 2002 dengue epidemic. We also acknowledge the contributions of Dr Chi-Tai Fang for his careful reviewing of this manuscript and valuable suggestions and endeavors of Ms Huei-Chu Chen, Ms Me-Chu Chen and Mr Chung-Hsin Huang for their assistance in epidemiological investigation, local laboratory diagnosis, and help in discussion. The research was supported by grants from the National Health Research Institute (NHRI-CN-CL9302P) and National Science Council (NSC #93-2320-B-002-074, NSC# 95-2314-B-002-274, NSC# 97-2314-B-002-180) in Taiwan. The authors also wish to acknowledge the administrative support of the joint program between the Department of Health and National Taiwan University Infectious Diseases Research and Education Center.

### Appendix A. Spatial autocorrelation and cluster detection

Spatial autocorrelation is the correlation of a variable in reference to spatial location of the variable. It can measure spatial clustering trends using statistical tests that can be characterized as *global* and *local* indices. Global indices are used to determine whether or not spatial clustering exists.<sup>23</sup> Local indices are employed to evaluate clustering trends of an attribute in each region by comparing whether the data are spatially similar or different and thus providing more information on the specific location of the testing clusters.<sup>24</sup>

#### A.1. Global test

Global tests of clustering detection are generally used to measure spatial autocorrelation coefficients by testing how clustered/dispersed the point locations are related to their attribute values. Spatial autocorrelation refers to the degree of similarity of attributes among the points within their neighborhood. Four situations are involved: (1) if there is any systematic pattern in the spatial distribution of a tested variable, it is said to be spatially auto-correlated; (2) if nearby or neighboring areas are more alike or points with similar characteristics tend to be near each other, this is called 'positive spatial autocorrelation'; (3) if patterns in which neighboring areas are unlike or nearby points have very dissimilar characteristics shown as disperse or uniform distribution of points, this is called 'negative autocorrelation'; and

(4) if random patterns of distribution occur when all the points do not exhibit any similar or dissimilar patterns, there is 'no spatial autocorrelation'.

The commonly used index to measure spatial autocorrelation is Moran's I. It is similar to Pearson's coefficient in that its numerator is a covariance while its denominator is a sample variance.<sup>22</sup> The mathematical formula is as follows:

$$I = \frac{N \sum_i \sum_j W_{ij} (X_i - \bar{X})(X_j - \bar{X})}{(\sum_i \sum_j W_{ij}) \sum_i (X_i - \bar{X})^2} \quad (2)$$

where  $N$  is the number of cases,  $\bar{X}$  is the mean of the variable,  $X_i$  is the variable value at a particular location  $i$ ,  $X_j$  is the variable value at another location  $j$ , and  $W_{ij}$  is a weight indexing location of  $i$  relative to  $j$ .

The value of Moran's I can range from  $-1$ , indicating a strong negative spatial autocorrelation, to  $+1$ , indicating a strong positive spatial autocorrelation. A value near  $0$  would indicate a spatially random pattern. Moran's I is a useful statistic because of its simplicity. However, its limitation is that it tends to average local variations in the strength of spatial autocorrelation, sometimes ignoring areas of local clustering. It requires further tests such as randomization or normal approximation to determine statistical significance.

## A.2. Local test

Tests for local indices evaluate spatial clustering trends in each region within the study area by comparing whether the data are spatially similar to or different from each other and thus providing more information on the location of clusters.<sup>23</sup> In our study, the local indicator of spatial autocorrelation (LISA) was used as the spatial risk index to identify both significant spatial clusters and outliers.<sup>24</sup> Spatial outliers refer to a certain area that has an opposite value to its neighboring areas, in contrast to spatial clusters with the similar value. Another, Getis and Ord's (1992) local spatial autocorrelation statistics,  $G_i^*(d)$  and  $G_i^*(d)$ , like LISA, was developed to search for local clustering patterns.<sup>22</sup> The mathematical formula is as follows:

$$G_i^*(d) = \frac{\sum_j w_{ij}(d) x_j}{\sum_j x_j} \quad (3)$$

where  $d$  is the neighborhood distance,  $x_j$  is the variable value at a particular location  $j$ , and  $w_{ij}$  is a weight indexing location of  $i$  relative to  $j$ . The  $G_i(d)$  statistic excludes the value at  $i$  from the summation and the  $G_i^*(d)$  includes the value at  $i$  in the summation and is often used for studies of clustering.

Local tests, such as  $G_i(d)$ ,  $G_i^*(d)$ , and LISA, can thus reveal the nature of spatial dependency in small localities. They can determine whether or not spatial patterns are statistically different from the null hypothesis – spatially randomly distributed – and whether these patterns represent clusters of low or high values.

## References

- [1] Snow J. On the mode of communication of cholera. The Commonwealth Fund. London: Oxford University Press; 1936.
- [2] Ali M, Wagatsuma Y, Emch M, Breiman RF. Use of geographic information system for defining spatial risk for dengue transmission in Bangladesh: role for *Aedes albopictus* in an urban outbreak. *Am J Trop Med Hyg* 2003;**69**:634–40.
- [3] Lai PC, Wong CM, Hedley AJ, Lo SV, Leung PY, Kong J, et al. Understanding the spatial clustering of severe acute respiratory syndrome (SARS) in Hong Kong. *Environ Health Perspect* 2004;**112**:1560–6.
- [4] Cockings S, Dunn CE, Bhopal RS, Walker DR. Users' perspectives on epidemiological, GIS and point pattern approaches to analyzing environment and health data. *Health Place* 2004;**10**:169–82.
- [5] Dunn CE, Kingham SP, Rowlingson B, Bhopal RS, Cockings S, Foy CJ, et al. Analysing spatially referenced public health data: a comparison of three methodological approaches. *Health Place* 2001;**7**:1–12.
- [6] Tran A, Deparis X, Dussart P, Morvan J, Rabarison P, Remy F, et al. Dengue spatial and temporal patterns, French Guiana, 2001. *Emerg Infect Dis* 2004;**10**:615–21.
- [7] Harrington LC, Scott TW, Lerdthusnee K, Coleman RC, Costero A, Clark GG, et al. Dispersal of the dengue vector *Aedes aegypti* within and between rural communities. *Am J Trop Med Hyg* 2005;**72**:209–20.
- [8] Morrison AC, Getis A, Santiago CM, Maciel JJ, Oliveira RM, Ribeiro MG, Amorim FP, et al. Exploratory space-time analysis of reported dengue cases during an outbreak in Florida, Puerto Rico, 1991–1992. *Am J Trop Med Hyg* 1998;**58**:287–98.
- [9] Siqueira JB, Martelli CM, Maciel JJ, Oliveira RM, Ribeiro MG, Amorim FP, et al. Household survey of dengue infection in central Brazil: spatial point pattern analysis and risk factors assessment. *Am J Trop Med Hyg* 2004;**71**:646–51.
- [10] Getis A, Morrison AC, Gray K, Scott TW. Characteristics of the spatial pattern of the dengue vector, *Aedes aegypti*, in Inquitos. *Peru Am J Trop Med Hyg* 2003;**69**:495–505.
- [11] Gubler DJ, Meltzer M. Impact of dengue/dengue hemorrhagic fever on the developing world. *Adv Virus Res* 1999;**53**:35–70.
- [12] World Health Organization. *Scientific working group report on dengue*. Geneva, Switzerland: TDR/WHO; 2006. Available at: [http://www.who.int/tdr/publications/publications/swg\\_dengue\\_2.htm](http://www.who.int/tdr/publications/publications/swg_dengue_2.htm) (accessed July 2009).
- [13] Bohra A, Andrianasolo H. Application of GIS in modeling of dengue risk based on sociocultural data: case of Jalore, Rajasthan. *India Dengue Bulletin* 2001;**25**:92–102.
- [14] Cummings DAT, Irizarry RA, Huang NE, Endy TP, Nisalak A, Ungchusak K, et al. Traveling waves in the occurrence of dengue hemorrhagic fever in Thailand. *Nature* 2004;**427**:344–7.
- [15] King CC, Wu YC, Chao DY, Kao CL, Wang HT, Chiang L, et al. Major epidemics of dengue in Taiwan in 1981–2000 related to the intensive virus activities in Asia and Public Health Surveillance. *Dengue Bulletin* 2000;**24**:1–10.
- [16] Kan CC, Lee PF, Wen TH, Chao DY, Wu MH, Lin NH, et al. Two clustering diffusion patterns identified from the 2001–2003 dengue epidemic. *Am J Trop Med Hyg* 2008;**79**:344–52.
- [17] Lanciotti RS, Calisher CH, Gubler DJ, Chang GJ, Vorndam AV. Rapid detection and typing of dengue viruses from clinical samples by using reverse transcriptase-polymerase chain reaction. *J Clin Microbiol* 1992;**30**:545–51.
- [18] Shu PY, Chen LK, Chang SF, Yueh YY, Chow L, Chien IJ, et al. Antibody to the nonstructural protein NS1 of Japanese encephalitis virus: potential application of mAb-based indirect ELISA to differentiate infection from vaccination. *Vaccine* 2001;**19**:1753–63.
- [19] Kuno G, Gubler DJ, Velez M, Oliver A. Comparative sensitivity of three mosquito cell lines for isolation of dengue viruses. *Bull World Health Organ* 1985;**63**:279–86.
- [20] Directorate General of Budget, Accounting and Statistics. *General report of the 2000 census of population and housing Taiwan-Fukien area, Republic of China*. Taiwan: DGBAS; 2000. Available at: <http://www.dgbas.gov.tw/> (in Chinese).(accessed July 2009).
- [21] Wen TH, Lin HN, Lin CH, King CC, Su MD. Spatial mapping of temporal risk characteristics to improve environmental health risk identification: a case study of a dengue epidemic in Taiwan. *Sci Total Environ* 2006;**367**:631–40.
- [22] Getis A, Ord JK. The analysis of spatial association by use of distance statistics. *Geogr Anal* 1992;**24**:189–206.
- [23] Odland J. Spatial autocorrelation. Newbury Park, CA: Sage; 1988.
- [24] Anselin L. Local indicators of spatial association—LISA. *Geogr Anal* 1995;**27**:93–115.
- [25] Lifson AR. Mosquitoes, models, and dengue. *Lancet* 1996;**347**:1201–2.
- [26] Chao DY, King CC, Wang WK, Chen WJ, Wu HL, Chang GJ. Strategically examining the full-genome of dengue virus type 3 in clinical isolates reveals its mutation spectra. *Virology* 2005;**24**:72.
- [27] Pinheiro FP, Corber SJ. Global situation of dengue and dengue haemorrhagic fever, and its emergence in the Americas. *World Health Stat Q* 1997;**50**:161–9.
- [28] Angel B, Joshi V. Distribution and seasonality of vertically transmitted dengue viruses in *Aedes* mosquitoes in arid and semi-arid areas of Rajasthan. *India J Vector Borne Dis* 2008;**45**:56–9.
- [29] Mermel LA. Pandemic avian influenza. *Lancet Infect Dis* 2005;**5**:666–7.